Activities of human exonuclease 1 that promote cleavage of transcribed immunoglobulin switch regions

Aarthy C. Vallur[a] and Nancy Maizels[a,b,1]

Departments of [a]Immunology and [b]Biochemistry, University of Washington Medical School, Seattle, WA 98195-7650

Edited by Richard D. Kolodner, University of California at San Diego School of Medicine, La Jolla, CA, and approved September 12, 2008 (received for review June 2, 2008)

Eukaryotic exonuclease 1 functions in replication, recombination, mismatch repair, telomere maintenance, immunoglobulin (Ig) gene class switch recombination, and somatic hypermutation. The enzyme has 5′–3′ exonuclease, flap endonuclease, and weak RNaseH activity *in vitro*, but it has been difficult to reconcile these activities with its diverse biological functions. We report robust cleavage by human exonuclease 1 of transcribed G-rich DNA sequences with potential to form G loops and G4 DNA. Predicted Ig switch recombination intermediates are substrates for both exonucleolytic and 5′ flap endonucleolytic cleavage. Excision is nick-dependent and structure-dependent. These results lead to a model for exonuclease 1 function in class switch recombination in which cleavage at activation-induced deaminase (AID)-initiated nicks produces gaps that become substrates for further attack by AID and subsequent repair.

antibody | B cell | cotranscriptional hybrid | G4 DNA | switch recombination

Eukaryotic exonuclease 1 (EXO1) belongs to class III of the RAD2 family of nucleases, which includes structure-specific nucleases like flap endonuclease 1 (FEN1). Purified recombinant human EXO1 (hEXO1) possesses 5′–3′ exonuclease activity on dsDNA, 5′ flap endonuclease activity, and weak RNaseH activity, and it is essential for both 5′ and 3′ nick-directed mismatch repair (1–4). In *Saccharomyces cerevisiae*, EXO1 functions in mismatch repair, replication, recombination, and at the telomeres (5–8). Mammalian EXO1 was identified as a homolog of *S. cerevisiae* Exo1p (1, 9) and by virtue of its interaction with hMSH2 (10). hEXO1 functionally complements its yeast homolog, and hEXO1 overexpression rescues conditional lethality of *S. cerevisiae rad27* (*FEN1*) mutants (2), suggesting some overlap of functions of EXO1 and FEN1. *Exo1*$^{-/-}$ mice display impaired meiosis, microsatellite instability, increased level of mutations and frequency of lymphomas (11), diminished efficiency of immunoglobulin (Ig) class switch recombination, and an altered spectrum of somatic hypermutation (12). In mice with dysfunctional telomeres, EXO1-deficiency extends life span and reduces genomic instability (13).

Class switch recombination is a regulated process of DNA deletion that joins a new constant region to the rearranged and expressed Ig heavy chain variable region in activated B cells (14–16). Recombination junctions are within switch (S) regions, 2- to 10-kb noncoding regions that are transcribed from a dedicated upstream promoter to activate recombination (Fig. 1*A*). Recombination is initiated by C to U deamination by the B cell-specific enzyme, activation-induced deaminase (AID), which preferentially deaminates within the consensus motif, WRCY (W = A/T, R = purine, Y = pyrimidine). AID-initiated damage is processed by redundant pathways, dependent on either uracil excision by UNG or mismatch recognition by MutSα (17). DNA nicking may then be promoted by the MRE11 AP lyase (18) or other AP endonucleases and lyases (19) or by factors that nick DNA for mismatch repair (4).

S regions contain G-rich repeats on the nontemplate DNA strand (Fig. 1*A*). Transcribed G-rich sequences, such as the S regions, form unusual stable structures, G loops, which contain an RNA/DNA hybrid on the template strand, and G4 DNA interspersed with single-stranded regions on the nontemplate strand (20, 21). Genetic evidence for EXO1 function at both the G-rich S regions (12) and the G-rich telomeric repeats (13) raised the possibility that EXO1 might excise structures formed in the course of transcription or replication. We have tested this by examining the activity of hEXO1 on transcribed DNA templates bearing Ig S region sequences. We report that predicted switch recombination intermediates are substrates for exonucleolytic digestion and for flap endonucleolytic cleavage, and excision depends on a G-rich nontemplate strand, an RNA/DNA hybrid on the C-rich template strand, and a DNA nick. These results identify an activity of hEXO1 at transcribed DNAs that may contribute to its function in class switch recombination and suggest a general mechanism for EXO1 function in determining stability of other G-rich genomic regions.

Results

Switch Junction Position Is Altered in *Exo1*$^{-/-}$ Mice. Switch recombination is region-specific, not sequence-specific, and produces chromosomal junctions that are typically heterogeneous in position (14, 15). Comparison of Sμ junction breakpoints in *Exo1*$^{-/-}$ and *Exo1*$^{+/-}$ mice revealed a modest difference in distribution, with median breakpoints at positions 218 and 272, respectively ($P = 0.11$, Student's t test). Comparison of Sγ3 junction breakpoints revealed a statistically significant difference, with median breakpoints at positions 2157 and 2344 respectively (Fig. 1*B*; $P = 1.2 \times 10^{-4}$, Student's t test). Thus, junctions in *Exo1*$^{-/-}$ mice mapped significantly closer to the upstream end of the Sγ3 region.

hEXO1 Can Function as Either an Exonuclease or Flap Endonuclease on Switch Substrates. To determine how EXO1 might function at transcribed S regions, we created substrates that recapitulate intermediates predicted to form at S regions activated for switch recombination. Several of the murine S regions, including Sμ, Sγ3, and Sα, comprise 2 sequence domains: AID deamination motifs (WRCY) cluster upstream, and G-rich repeats downstream (Fig. 1*A*). After transcription, the upstream region will reanneal to form dsDNA, whereas the downstream G-rich region is predicted to form a G loop, containing a stable

Author contributions: A.C.V. and N.M. designed research; A.C.V. performed research; A.C.V. and N.M. analyzed data; and A.C.V. and N.M. wrote the paper.

The authors declare no conflict of interest.

This article is a PNAS Direct Submission.

[1]To whom correspondence should be addressed at: Department of Immunology, HSB H474A, University of Washington Medical School, 1959 NE Pacific Street, Box 357650, Seattle, WA 98195-7650. E-mail: maizels@u.washington.edu.

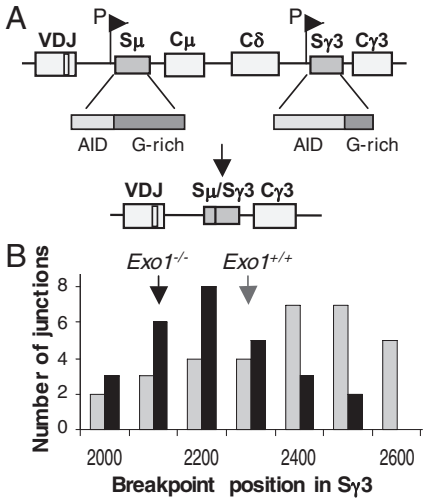

Fig. 1. Switch junctions are altered in *Exo1*$^{-/-}$ mice. (*A*) Switch recombination from μ to γ3. Shown is a portion of the murine IgH locus before (*Upper*) and after (*Lower*) switch recombination. Domains of Sμ and Sγ3 that are rich in AID motifs or G runs are indicated (*Middle*). Variable (VDJ); switch (S); constant (C); S region promoters (P). (*B*) Comparison of switch junction breakpoint positions in the Sγ3 region of IgG3^{+} B cells from *Exo1*$^{+/-}$ (light bars) and *Exo1*$^{-/-}$ (dark bars) mice. Junction sequences (12) were aligned to the GenBank Sμ sequence (MUSIGD07) or Sγ3 sequence (MUSIGHANA) and binned in 100-bp intervals with upstream end at the position indicated. Arrows denote median for each dataset. Differences between medians are significant ($P = 1.2 \times 10^{-4}$, Student's *t* test).

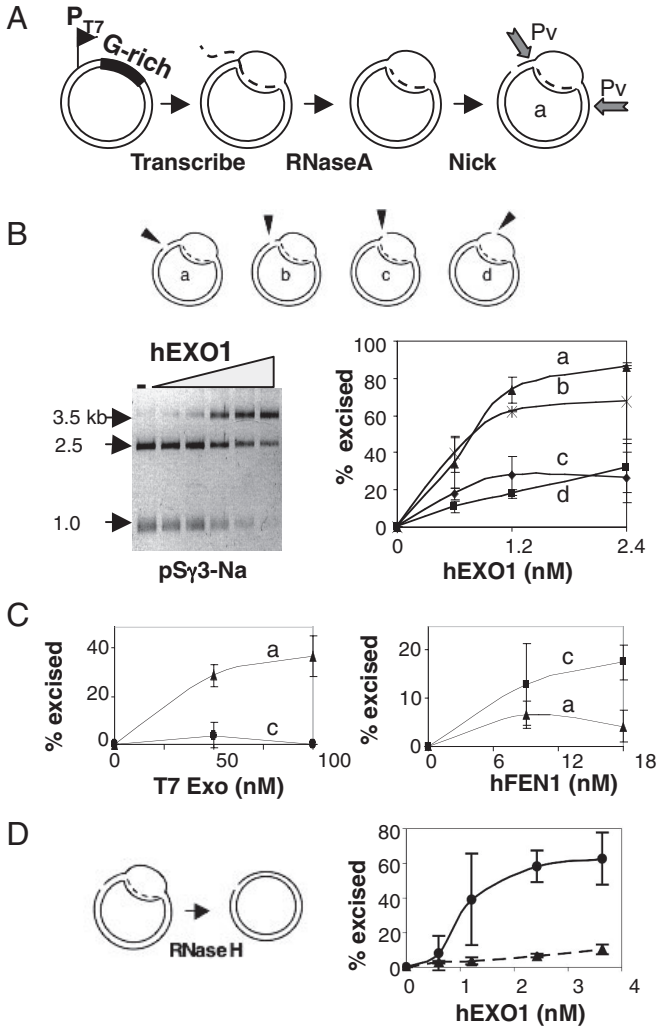

Fig. 2. hEXO1 excision of Sγ3 substrates. (*A*), pSγ3-N switch substrate before and after transcription, RNaseA treatment, and nicking. P_{T7}, T7 promoter; dark fill, 600-bp G-rich region from murine Sγ3; dashed line, RNA transcript; open arrows, PvuII cleavage sites (Pv). (*B*) (*Upper*) Diagrams of plasmids nicked within dsDNA (pSγ3-Na, pSγ3-Nb) or the single-stranded G loop (pSγ3-Nc, pSγ3-Nd). (*Lower*) (*Left*) Agarose gel electrophoresis of products of hEXO1 (0, 0.6, 1.2, 2.4, 3.6, and 4.8 nM) digestion of transcribed and nicked pSγ3-Na substrates, which contain two PvuII sites (see *A*). (*Right*) Quantitation of hEXO1 (0, 0.6, 1.2, and 2.4 nM) activity on transcribed, RNaseA-treated, and nicked pSγ3-Na (triangles), pSγ3-Nb (crosses), pSγ3-Nc (diamonds), and pSγ3-Nd (squares), labeled *a*–*d* in the graph. (*C*) Quantitation of T7 Exo (*Left*) and hFEN1 (*Right*) activity on pSγ3-Na (triangles) and pSγ3-Nc (circles) substrates, transcribed, treated with RNaseA, and nicked. (*D*) (*Left*) RNaseH treatment causes collapse of a G loop. (*Right*) Quantitation of hEXO1 (0, 0.6, 1.2, 2.4, and 3.6 nM) activity on pSγ3-Na substrates, transcribed, treated with RNaseA, and nicked, and then untreated (circles) or treated with RNaseH (triangles) before incubation with hEXO1.

RNA/DNA hybrid on the template strand and G4 DNA interspersed with single-stranded regions on the nontemplate strand. AID-initiated nicks could be located in either the duplex or single-stranded region, presenting distinct structures for subsequent processing, and switch substrates were therefore designed to assay activities of EXO1 on substrates containing nicks within either dsDNA or ssDNA. Switch substrates carried a T7 promoter upstream of a 600-bp G-rich region derived from the murine Sγ3 switch region; an Nb.BbvC1 nicking site either in the region predicted to remain duplex after transcription (pSγ3-Na, pSγ3-Nb) or in the G-rich region, where transcription-induced G loops are predicted to form (pSγ3-Nc and pSγ3-Nd); and a diagnostic restriction site downstream of the nicking site. Substrates were transcribed *in vitro* with T7 polymerase; and after free RNA was digested with RNaseA, DNA was nicked with Nb.BbvC1 (Fig. 2*A*). Control experiments verified that templates were supercoiled and that transcription, RNaseA digestion, and nicking were efficient (data not shown).

hEXO1 digestion assays took advantage of the fact that either excision from a nick or endonucleolytic cleavage of a flap will convert dsDNA to ssDNA and thereby prevent cleavage by restriction enzymes that recognize dsDNA but not ssDNA. Transcribed and nicked substrates (Fig. 2*B Upper*) were incubated with hEXO1, treated with RNaseH to promote renaturation of the duplex, subjected to diagnostic restriction cleavage, and DNA fragments were resolved by native gel electrophoresis and quantified. Analysis of pSγ3-Na, which carries a diagnostic PvuII site 31 bp downstream of the nick (Fig. 2*A Right*), showed that before hEXO1 digestion PvuII cleaved the intact plasmid to generate fragments 2.5 and 1.0 kb in length and that the fraction of PvuII-resistant 3.5-kb product increased with increasing amounts of hEXO1 (Fig. 2*B Left*). Comparison of hEXO1 digestion of transcribed and nicked pSγ3-Na, pSγ3-Nb, pSγ3-Nc, and pSγ3-Nd showed that, although hEXO1 was active on all four substrates, it was 2.5- to 4-fold more active on substrates pSγ3-Na and pSγ3-Nb (Fig. 2*B Right*) in which the nick is within the duplex region. Consistent with this, T7 Exo, which can excise from a nick or gap in duplex DNA (22), was active on nicked pSγ3-Na but not pSγ3-Nc (Fig. 2*C Left*). In contrast, the nick in pSγ3-Nc and pSγ3-Nd is in the G loop, creating structures that would be predicted to be substrates for 5′ flap endonuclease activity. Consistent with this, the well-characterized human 5′ flap endonuclease, hFEN1 (23), was active on pSγ3-Nc but relatively inactive on pSγ3-Na (Fig. 2*C Right*).

hEXO1 Excision Depends on the Presence of a G Loop. Dependence of excision on a G loop was tested by treating transcribed and

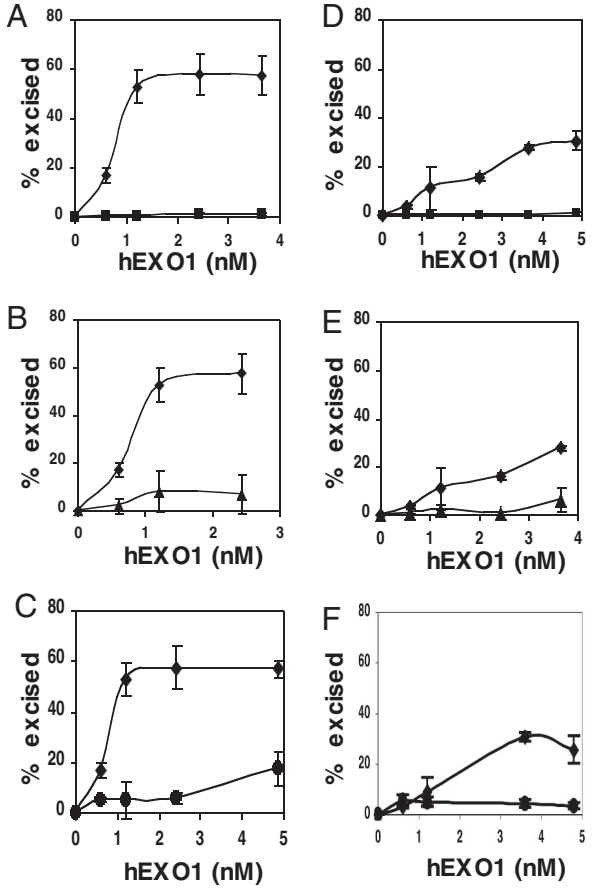

Fig. 3. hEXO1 excision of S region substrates is nick-directed and transcription- and orientation-dependent. (*A*) hEXO1 (0, 0.6, 1.2, 2.4, and 3.6 nM) activity on transcribed pSγ3Na, either unnicked (boxes) or nicked with Nb.BbvC1 (diamonds) after transcription. (*B*) hEXO1 (0, 0.6, 1.2, and 2.4 nM) activity on nicked pSγ3-Na, transcribed (diamonds) or untranscribed (triangles). (*C*) hEXO1 (0, 0.6, 1.2, 2.4, and 4.8 nM) activity on transcribed and nicked pSγ3-Na (diamonds) or pSγ3R-Na (circles). (*D*) hEXO1 (0, 0.6, 1.2, 2.4, 3.6, and 4.8 nM) on transcribed pSμ-N, either unnicked (boxes) or nicked with Nb.BbvC1 (diamonds) after transcription. (*E*) hEXO1 (0, 0.6, 1.2, 2.4, and 3.6 nM) activity on nicked pSμ-N, either transcribed (diamonds) or untranscribed (triangles). (*F*) hEXO1 (0, 0.6, 1.2, 3.6, and 4.8 nM) activity on transcribed and nicked pSμ-N (diamonds) or pSμR-N (circles).

nicked pSγ3-Na with RNaseH, which digests the RNA strand of an RNA/DNA hybrid, causing G loops to collapse (20; Fig. 2*D*, (*Left*). RNaseH digestion protected the DNA from excision by hEXO1 (Fig. 2*D Right*). Thus, hEXO1 excision depends on the G loop structure.

hEXO1 Excision Requires a Nick. Dependence of excision on a nick was assayed by comparing digestion of nicked and unnicked transcribed pSγ3-Na substrates, quantitating digestion by indirect labeling. Approximately 60% of nicked substrate molecules were excised by 1.2 nM hEXO1, but unnicked substrates were not digested (Fig. 3*A*). Thus, hEXO1 requires a nick 5′ of the target region.

hEXO1 Excision Depends on Transcription and Transcriptional Orientation. Dependence of excision on transcription was tested by comparing hEXO1 activity on pSγ3-Na substrates that had been either transcribed or not transcribed before nicking. Untranscribed substrates were very poorly digested compared with transcribed substrates (Fig. 3*B*). Thus, nicking alone is not sufficient to make the DNA a good substrate for hEXO1.

Efficient class switch recombination requires transcription of the S regions in the physiological orientation, with a G-rich nontemplate and C-rich template strand (24); and formation of G loops and G4 DNA by transcribed G-rich substrates is similarly orientation-dependent (20). Comparison of hEXO1 activity on transcribed and nicked pSγ3-Na and the analogous substrate, pSγ3-RNa, in which the orientation of the Sγ3 repeat was reversed, showed that robust activity was evident only if the nontemplate strand was G-rich, the orientation permissive for G loop formation (Fig. 3*C*).

Nick-Dependent, Orientation-Dependent Excision of Sμ Repeats by hEXO1. To establish whether other G-rich regions can serve as substrates for hEXO1, we tested hEXO1 activity on substrates pSμ-N and pSμ-RN, which carry a 300-bp insert bearing tandem repeats of the 20-mer G-rich Sμ consensus sequence, in forward and reverse orientations, respectively, and an Nb.BbvC1 site 191 nt upstream of the Sμ boundary, so that nicking will occur within duplex DNA (as in pSγ3-Na and pSγ3-RNa, above). Excision was nick-dependent (Fig. 3*D*) and transcription-dependent (Fig. 3*E*). Robust exonuclease activity was evident if the Sμ repeats were in the forward (pSμ-N) but not in the reverse (pSμ-RN) orientation (Fig. 3*F*). Thus, dependence of hEXO1 cleavage on nicking, transcription, and S region orientation on the Sμ substrate was comparable with that observed with the Sγ3 substrate (Fig. 3 *A–C*). We note that the fraction of pSμ-N substrates excised was consistently lower, with a maximum in the range of 35–40%, rather than 60–65% typically observed for the pSγ3-Na substrates. This may reflect the fact that the Sμ template is shorter and less G-rich than the Sγ3 template and forms G loops less readily.

hEXO1 Flap Endonuclease Activity May Cleave Within G Loops. To confirm that the 5′ flap endonuclease activity of hEXO1 can digest substrates containing an RNA/DNA hybrid at the junction of the duplex and the 5′ flap, as suggested by results in Fig. 2, we generated synthetic 5′ flap substrates in which a 5′ end-labeled 16-nt flap was adjacent to a either a DNA/DNA or RNA/DNA hybrid (Fig. 4*A*). After treatment with hEXO1, the 16-nt flap was released with comparable efficiency from both substrates (Fig. 4*B*). The ability of the hEXO1 flap endonuclease to remove 5′ flaps adjacent to RNA/DNA hybrids would enable it to remove one arm of a nicked G loop.

Switch recombination is impaired but not abolished in *Exo1*$^{-/-}$ mice (12), suggesting that there may be activities that overlap with EXO1 in living cells, and results in Fig. 2*D* identify FEN1 as a candidate activity. Assays on synthetic substrates confirmed that, like hEXO1, hFEN1 can efficiently remove 5′ flaps adjacent to RNA/DNA hybrids (Fig. 4*C*).

Discussion

We have demonstrated that hEXO1 cleaves transcribed substrates carrying G-rich inserts from the Ig switch regions, acting as either an exonuclease or a 5′ flap endonuclease. Cleavage requires a nick, either upstream of or within the G-rich region. After transcription, a nick upstream of the G-rich region provides a free 5′ end within the DNA duplex, which is a substrate for excision; whereas a nick within the G-rich region creates a 5′ flap, which is a substrate for endonucleolytic cleavage.

Both the exonuclease and flap endonuclease activities of EXO1 may contribute to its function in Ig heavy chain class switch recombination. Switch recombination depends on S region transcription, which produces stable RNA/DNA hybrids, identified at the S regions of activated B cells (25); and it is region-specific but not site-specific, reflecting in part the ability of AID to attack at many different sites within an S region. AID preferentially deaminates ssDNA, and if nicking occurs before renaturation of the duplex, the nick will be within a single-

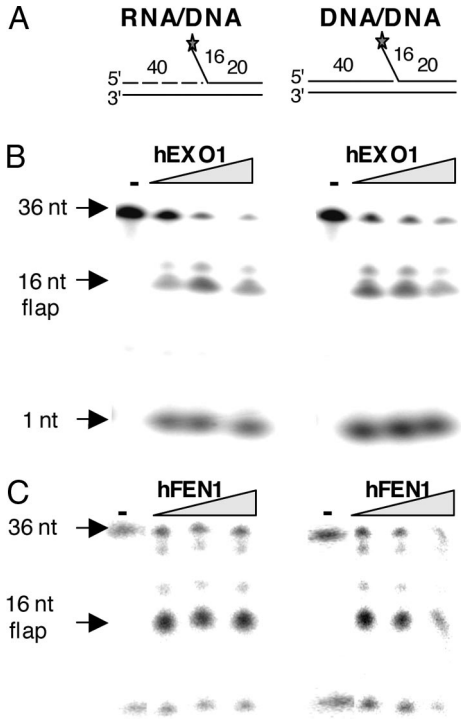

Fig. 4. Cleavage of 5′ flap substrates containing RNA/DNA or DNA/DNA hybrids by hEXO1 and hFEN1. (*A*) Diagram of 5′ flap substrates, which contained a 40-nt RNA/DNA (*Left*) or DNA/DNA (*Right*) hybrid and a 16-nt 5′-end-labeled flap (numbers denote fragment lengths, dotted line denotes RNA, asterisk denotes labeled end). (*B*) Products of cleavage by hEXO1 (0, 1.2, 2.4, and 3.6 nM) of flap substrates containing RNA/DNA (*Left*) or DNA/DNA (*Right*) hybrids, resolved by 20% acrylamide denaturing gel electrophoresis; arrows indicate 36-nt substrate, 16-nt flap, and 1-nt exonuclease products. (*C*) Products of cleavage of flap substrates by hFEN1 (0, 4.5. 9, and 18 nM); notations as in *B*. The fast-migrating trace of radioactivity is unincorporated label and not the result of exonucleolytic digestion, as it is also evident in the undigested control lanes (–, no enzyme).

stranded region; however, if a transcribed S region reanneals subsequent to deamination but before nicking, the nick will be within dsDNA. Thus, nicks may be present either in single-stranded or duplex DNA within regions activated for recombination *in vivo*. hEXO1 was severalfold more active on transcribed substrates with nicks within dsDNA than ssDNA. Excision from a nick in dsDNA required that the substrates be transcribed in the physiological orientation, which induces formation of G loops. This orientation dependence suggests that hEXO1 may recognize one or more components of the G loop structure.

The 5′ flap endonuclease activity of hEXO1 supported cleavage of substrates bearing nicks in ssDNA. The ability of hEXO1 to release a 5′ flap adjacent to an RNA/DNA hybrid, like those formed in transcribed S regions, raises the interesting possibility that EXO1 may act at other stable cotranscriptional RNA/DNA hybrids, which can be a source of genomic instability (26). We found that, like hEXO1, hFEN1 can cleave flaps adjacent to RNA/DNA hybrids, suggesting that FEN1 may have overlapping functions in such repair pathways. Overlapping activities of FEN1 and EXO1 *in vivo* are consistent with evidence that overexpression of EXO1 can rescue conditional lethality of *S. cerevisiae* RAD27 (FEN1) mutants (2).

Fig. 5 presents a very simple working model for how EXO1 may contribute to switch recombination. This model postulates that EXO1 initiates at a nick and removes a region of the G-rich nontemplate strand, either by excision (above) or flap endonucleolytic cleavage (below). The RNA/DNA hybrid is shown as persisting during excision because its removal by treatment with exogenous RNaseH prevented digestion of the DNA. [EXO1 itself has RNaseH activity (2), but because this did not interfere with excision of switch substrates, so in contrast to exogenous RNaseH, it may be weak relative to the DNA digestion activities documented.] After EXO1 digestion of a portion of the nontemplate strand, removal of the RNA/DNA hybrid by cellular activities would expose a single-stranded gap on the C-rich template strand, which may itself be a target for AID, or may be bound by RPA, which stimulates AID (27). By exposing the C-rich strand to attack by AID, EXO1 would increase the overall efficiency of switch recombination, as it has been shown to do (12). A second cycle of deamination and nicking of the template strand would in effect generate a double-strand break (DSB) that provides one side of a recombination junction. Joining of this DSB to a partner in another switch region, mediated by the nonhomologous end-joining pathways, would create the heterogeneous junctions characteristic of switch recombination.

The model suggests that the EXO1 exonuclease and flap endonuclease activities might contribute differently to switch junction position, with the exonuclease activity predominately excising from nicks in AID-rich regions, and the flap endonuclease activity cleaving within G-rich regions which have formed G-loops. The overlapping activities of hEXO1 and hFEN1 at flaps adjacent to RNA/DNA hybrids suggest that, in the absence of EXO1, FEN1 could support switch recombination, albeit at reduced efficiency, because FEN1 can cleave at flaps but not excise.

This working model may also provide insight into the roles of MLH1 and PMS2, the two components of MutLα, in formation of microhomologies at switch junctions. Switch junction microhomologies are 1–2 nt in length in wild-type mice (12, 28, 29) and from 3 to 10 nt in length in *Mlh1*$^{-/-}$ (30) and *Pms2*$^{-/-}$ mice (28). MutLα limits hEXO1 activity and excision tract lengths in 5′ mismatch repair reconstituted *in vitro* (31). By analogy, the

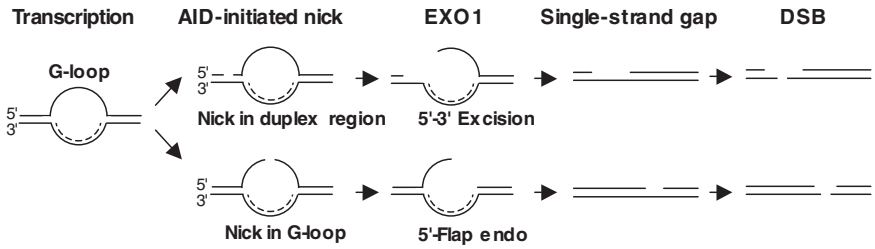

Fig. 5. Working model for hEXO1 excision at transcribed S regions. (*Upper*) A transcribed S region is nicked in duplex DNA and then undergoes excision by the EXO1 5′-3′ exonuclease activity. (*Lower*) A transcribed S region is cleaved by the 5′-flap endonuclease activity. In both cases, a single-strand gap is generated which is a target for subsequent AID-initiated nicking, resulting in DSBs that are joined by nonhomologous end-joining to form switch junctions. See *Discussion* for details.

absence of MLH1 or PMS2 may promote excision by EXO1 at S regions, making longer regions of resected ssDNA available for homology-dependent interactions.

Excision by hEXO1 may also contribute to genomic stability, or instability, at G-rich regions of the genome other than the S regions. Sites of recurrent translocations have been shown to cluster in G-rich regions with potential to form G4 DNA in the c-*MYC*, *BCL6*, *RhoH*, *PIM1*, and *PAX5* protooncogenes in AID-positive B cell tumors (21, 32). These genes are all actively transcribed in the cell types in which they are prone to translocation and may provide targets for EXO1 analogous to those at the transcribed G-rich S regions.

Materials and Methods

Plasmids. pSγ3-N, a derivative of pPH600 (20), carries a 600-bp fragment from the murine Sγ3 region cloned into the BamHI and HindIII sites of the pBluescript(KS+) vector, downstream of the T7 promoter (Fig. 2). pSγ3-Na, pSγ3-Nb, pSγ3-Nc, and pSγ3-Nd were generated by using QuikChange (Stratagene) to incorporate sites for the Nb.BbvC1 nickase at positions -191, -139, $+31$, or $+336$ relative to the Sγ3 upstream boundary, and with diagnostic restriction sites 31 bp 3′ of the nick site. pSγ3R-Na is identical to pSγ3-Na but carries the Sγ3 insert in the reverse orientation. pSμ-N and pSμ-RN are analogous to pSγ3-Na and pSγ3R-Na but contain repeats of a synthetic Sμ 20-mer in place of Sγ3 sequences. Plasmid constructs were verified by sequencing.

Enzymes. The baculovirus expressing human exonuclease 1b (hEXO1b, referred to as hEXO1 herein) was a kind gift from Paul Modrich (Duke University Medical Center, Durham, NC). hEXO1 was expressed in insect Sf9 cells by the National Center for Cell Culture (Minneapolis, MN); purified as in ref. 3; and exonuclease activity was verified (data not shown). Protein concentrations were determined by Bradford assay. hEXO1 was diluted in 7.5 mM Hepes (pH 7.5), 200 mM KCl, 0.6 mM DTT, 2 mg/ml BSA, and 10% (vol/vol) glycerol. hEXO1 preparations were tested for contaminating endonucleases by incubation with 1.4 nM supercoiled plasmids in 20-μL reactions for 30 min at 37 °C (data not shown). Digestions with hFEN1 (Trevigen) and T7 Exo (NEB) were carried out in 20-μL reactions as specified by the suppliers.

hEXO1 Substrates and Assays. Plasmids were transcribed in 30-μL reactions containing 40 mM KCl, 0.5 mM each NTP, 10 mM DTT, 140 nM plasmid DNA, 50 units of T7 RNA polymerase (NEB), and manufacturer's buffer at 37 °C for 15 min. Products were incubated with 5 μg of RNaseA (Fermentas) at 37 °C for 15 min to digest free RNA transcripts, then nicked with 10 units of Nb.BbvC1 (NEB) at 37 °C for 60 min, phenol-extracted, ethanol-precipitated, resuspended at 1.4 nM DNA in 40 mM Tris·HCl (pH 7.6), 2 mM glutathione, 10 mM $MgCl_2$, and 0.1 mg/ml BSA; and 10-μL aliquots were incubated with hEXO1 at 37 °C for 15 min. In all cases, control experiments verified efficiency of transcription, RNaseA digestion, and nicking. RNaseH digestion was carried out in 10-μL reactions containing 1.4 nM DNA substrate and 2 units of RNaseH (Fermentas) in manufacturer's buffer at 37 °C for 20 min. Reactions were extracted with phenol then chloroform, 1 μg of glycogen carrier (Sigma) was added, and DNA was ethanol-precipitated and resuspended in restriction buffer. pSγ3-Na and pSγ3-Nb were resuspended in 1× buffer G (Fermentas), and pSγ3-Nc and pSγ3-Nd in 1× buffer O (Fermentas). Substrates were digested with 0.5 unit of RNaseH at 37 °C for 20 min to remove RNA/DNA hybrids and enable efficient restriction digestion, then cleaved with 10 units of restriction enzyme at 37 °C for 1 h: PvuII for pSγ3-Na, AflIII (NEB) for pSγ3-Nb and pSγ3-Nc, and BamHI (NEB) and AflIII for pSγ3-Nd. DNA was resolved by 1% agarose gel electrophoresis, imaged after ethidium bromide staining, transferred in 0.5 M NaOH to Zeta-probe nylon membranes (Bio-Rad), and hybridized with a 5′ ^{32}P-labeled oligonucleotide complementary to the nontemplate strand of the insert for indirect labeling (33). After PhosphorImaging and quantitation using ImageQuant software (Amersham), exonuclease activity was calculated as the ratio of the 3.5-kb PvuII-resistant fragment to total DNA. Flap substrates were generated by annealing the 60-mer complement 5′-d(TAGCGACTAGACGGGGAAAGCCGAATTTCTAGAATCGAAAGCTTGCTAGCAATTCGGCGA) to the flap 36-mer, 5′-d(ATCATGGCTTGCGATACTTTCCCCGTCTAGTCGCTA); and a 40-mer composed of either DNA [5′-d(GCTAGCAAGCTTTCGATTCTAGAAATTCGGCTTTCCCCGC)], or RNA [5′-r(GCUAGCAAGCUUUCGAUUCUAGAAAUUCGGCUUUCCCCGC)].

ACKNOWLEDGMENTS. We thank all members of the Maizels laboratory for valuable discussions. This work was supported by National Institutes of Health Grants R01 GM39799 and R01 GM65988 (to N.M.).

1. Wilson DM, 3rd, *et al*. (1998) Hex1: A new human Rad2 nuclease family member with homology to yeast exonuclease 1. *Nucleic Acids Res* 26:3762–3768.
2. Qiu J, Qian Y, Chen V, Guan MX, Shen B (1999) Human exonuclease 1 functionally complements its yeast homologues in DNA recombination, RNA primer removal, and mutation avoidance. *J Biol Chem* 274:17893–17900.
3. Genschel J, Bazemore LR, Modrich P (2002) Human exonuclease I is required for 5′ and 3′ mismatch repair. *J Biol Chem* 277:13302–13311.
4. Kunkel TA, Erie DA (2005) DNA mismatch repair. *Annu Rev Biochem* 74:681–710.
5. Lewis LK, Westmoreland JW, Resnick MA (1999) Repair of endonuclease-induced double-strand breaks in *Saccharomyces cerevisiae*: Essential role for genes associated with nonhomologous end-joining. *Genetics* 152:1513–1529.
6. Maringele L, Lydall D (2002) EXO1-dependent single-stranded DNA at telomeres activates subsets of DNA damage and spindle checkpoint pathways in budding yeast yku70Delta mutants. *Genes Dev* 16:1919–1933.
7. Bertuch AA, Lundblad V (2004) EXO1 contributes to telomere maintenance in both telomerase-proficient and telomerase-deficient *Saccharomyces cerevisiae*. *Genetics* 166:1651–1659.
8. Tran PT, Erdeniz N, Symington LS, Liskay RM (2004) EXO1: A multitasking eukaryotic nuclease. *DNA Repair* 3:1549–1559.
9. Tishkoff DX, Amin NS, Viars CS, Arden KC, Kolodner RD (1998) Identification of a human gene encoding a homologue of *Saccharomyces cerevisiae* EXO1, an exonuclease implicated in mismatch repair and recombination. *Cancer Res* 58:5027–5031.
10. Schmutte C, *et al*. (1998) Human exonuclease I interacts with the mismatch repair protein hMSH2. *Cancer Res* 58:4537–4542.
11. Wei K, *et al*. (2003) Inactivation of exonuclease 1 in mice results in DNA mismatch repair defects, increased cancer susceptibility, and male and female sterility. *Genes Dev* 17:603–614.
12. Bardwell PD, *et al*. (2004) Altered somatic hypermutation and reduced class-switch recombination in exonuclease 1-mutant mice. *Nat Immunol* 5:224–229.
13. Schaetzlein S, *et al*. (2007) Exonuclease-1 deletion impairs DNA damage signaling and prolongs lifespan of telomere-dysfunctional mice. *Cell* 130:863–877.
14. Chaudhuri J, Alt FW (2004) Class-switch recombination: Interplay of transcription, DNA deamination, and DNA repair. *Nat Rev Immunol* 4:541–552.
15. Maizels N (2005) Immunoglobulin gene diversification. *Annu Rev Genet* 39:23–46.
16. Vallur AC, Yabuki M, Larson ED, Maizels N (2007) AID in antibody perfection. *Cell Mol Life Sci* 64:555–565.
17. Rada C, Di Noia JM, Neuberger MS (2004) Mismatch recognition and uracil excision provide complementary paths to both Ig switching and the A/T-focused phase of somatic mutation. *Mol Cell* 16:163–171.
18. Larson ED, Cummings WJ, Bednarski DW, Maizels N (2005) MRE11/RAD50 cleaves DNA in the AID/UNG-dependent pathway of immunoglobulin gene diversification. *Mol Cell* 20:367–375.
19. Ramiro A, *et al*. (2007) The role of activation-induced deaminase in antibody diversification and chromosome translocations. *Adv Immunol* 94:75–107.
20. Duquette ML, Handa P, Vincent JA, Taylor AF, Maizels N (2004) Intracellular transcription of G-rich DNAs induces formation of G loops, novel structures containing G4 DNA. *Genes Dev* 18:1618–1629.
21. Duquette ML, Huber MD, Maizels N (2007) G-rich proto-oncogenes are targeted for genomic instability in B-cell lymphomas. *Cancer Res* 67:2586–2594.
22. Kerr C, Sadowski PD (1972) Gene 6 exonuclease of bacteriophage T7. I. Purification and properties of the enzyme. *J Biol Chem* 247:305–310.
23. Bambara RA, Murante RS, Henricksen LA (1997) Enzymes and reactions at the eukaryotic DNA replication fork. *J Biol Chem* 272:4647–4650.
24. Shinkura R, *et al*. (2003) The influence of transcriptional orientation on endogenous switch region function. *Nat Immunol* 4:435–441.
25. Yu K, Chedin F, Hsieh CL, Wilson TE, Lieber MR (2003) R-loops at immunoglobulin class switch regions in the chromosomes of stimulated B cells. *Nat Immunol* 4:442–451.
26. Li X, Manley JL (2006) Cotranscriptional processes and their influence on genome stability. *Genes Dev* 20:1838–1847.
27. Chaudhuri J, Khuong C, Alt FW (2004) Replication protein A interacts with AID to promote deamination of somatic hypermutation targets. *Nature* 430:992–998.
28. Ehrenstein MR, Rada C, Jones AM, Milstein C, Neuberger MS (2001) Switch junction sequences in PMS2-deficient mice reveal a microhomology-mediated mechanism of Ig class switch recombination. *Proc Natl Acad Sci USA* 98:14553–14558.
29. Schrader CE, Vardo J, Stavnezer J (2003) Mlh1 can function in antibody class switch recombination independently of Msh2. *J Exp Med* 197:1377–1383.
30. Schrader CE, Vardo J, Stavnezer J (2002) Role for mismatch repair proteins Msh2, Mlh1, and Pms2 in immunoglobulin class switching shown by sequence analysis of recombination junctions. *J Exp Med* 195:367–373.
31. Zhang Y, *et al*. (2005) Reconstitution of 5′-directed human mismatch repair in a purified system. *Cell* 122:693–705.
32. Duquette ML, Pham P, Goodman MF, Maizels N (2005) AID binds to transcription-induced structures in c-MYC that map to regions associated with translocation and hypermutation. *Oncogene* 24:5791–5798.
33. Au KG, Welsh K, Modrich P (1992) Initiation of methyl-directed mismatch repair. *J Biol Chem* 267:12142–12148.